# Numerical Analysis for the Adiabatic Demagnetization Refrigerator (ADR) Operating between 4.5 K and 2.0 K

**D. Kwon, J. Bae, and S. Jeong.**

Cryogenic Engineering Laboratory, Mechanical Engineering Dept.,
School of Mechanical and Aerospace Engineering,
Korea Advanced Institute of Science and Technology,
291, Daejeon, Rep. of Korea

## ABSTRACT

An adiabatic demagnetization refrigerator (ADR) is numerically investigated to predict the cooling performance below 4.5 K. The proposed system consists of helium thermosyphon for the warm side heat switch and a magneto-resistive tungsten for the cold side heat switch. Gadolinium Gallium Garnet (GGG) is selected as magnetic material. By adapting appropriate heat switching method for the warm and the cold sides, the passive operation of heat switches is feasible. The numerical analysis is conducted with the 1-dimensional heat diffusion model considering thermal contact resistance in ADR. Homogeneous model is applied on the thermosyphon heat switch. The calculation results show that the ADR can produce cooling capacity of 0.770 J at 2 K when the temperature of the warm end is maintained as 4.5 K. COP of the ADR is predicted as 0.376. The detailed design methodology and the results are presented and discussed.

## INTRODUCTION

Magnetocaloric effect (MCE), which is firstly discovered by Warburg, is the phenomenon that the temperature or the entropy of the magnetic material is changed by variation of magnetic field. This phenomenon is caused by interaction between magnetic moments inside the magnetic material and magnetic field. With MCE, it is possible to create cooling effect by 'magnetically compress or expand' the magnetic material with alternating field. This is a fundamental principle of magnetic refrigeration, which was firstly proposed by Giauque [1] and Debye [2]. Adiabatic demagnetization refrigerator (ADR) is one type of the magnetic refrigeration. The ADR can achieve temperature lower than 1 K which cannot be achieved by conventional gas-compression refrigerator [3].

Heat switch is a device that adjusts its heat transfer 'state' to turn on or off at proper intervals. Since the temperature of the magnetic material continuously alternates during the ADR cycle, the heat switch must regulate the thermal connection harmoniously between the magnetic material and the warm end or the cold end of the system. Bywaters and Griffin [4] proposed gas-gap heat switch that regulate its state by utilizing the presence of gas between narrow gap. Gas is filled to or evacuated from the gap by getter which has a characteristic of adsorbing gas. Heat switches are usually actively controlled to regulate their states, thus additional control system for heat switch is required increasing system complexity. In the case of the

*Cryocoolers 21,* edited by R.G. Ross, Jr., J.R. Raab and S.D. Miller

**Table 1.** Analysis Nomenclature

| | | | |
|---|---|---|---|
| A | area ($m^2$) | | **Greek** |
| B | magnetic flux density (T) | $\rho$ | density ($kg/m^3$) |
| $c_P$ | specific heat at constant pressure (J/kg K) | $\mu$ | viscosity (Pa-s) |
| $c_H$ | specific heat at constant field strength (J/kg K) | $\mu_0$ | permeability ($4\pi \times 10^{-7}$ H/m) |
| $g$ | gravitational acceleration (9.81 $m/s^2$) | $\sigma$ | surface tension (N/m) |
| $H$ | magnetic field strength (A/m) | | **Subscripts** |
| $h$ | heat transfer coefficient ($W/m^2$ K) | $c$ | condenser |
| $i_{lg}$ | latent heat of vaporization (J/kg) | *C.E.* | cold end |
| $k$ | thermal conductivity (W/m K) | $e$ | evaporator |
| L | length (m) | *el* | electron |
| $M$ | magnetization (A/m) | $g$ | gas |
| $m$ | mass (kg) | $l$ | liquid |
| $P$ | pressure (Pa) | *max.* | maximum |
| $Q$ | heat energy (J) | *min.* | minimum |
| $\dot{Q}$ | heat transfer rate (W) | *ph* | phonon |
| s | specific entropy (J/kg K) | *sat.* | saturated |
| $T$ | temperature (K) | *sys.* | system |
| $t$ | time (s) | *W.E.* | warm end |
| u | specific internal energy (J/kg) | | |
| $V$ | volume ($m^3$) | | |
| $v$ | specific volume ($m^3$/kg) | | |

gas-gap heat switch, its state was controlled by installing a heater on the getter in order to adjust its adsorption capacity of getter [5]. If the heat switch passively operates without additional control system, the whole refrigeration system can be simplified. Subsequently, a passive gas-gap heat switch was also investigated to simplify the system by DiPirro et al. [6] and Kimball et al. [7]. The heat switch can passively operate without the additional heater by means of contacting the getter with magnetic material which alternates its temperature during refrigeration cycle. However, there is a disadvantage that the operation speed of the heat switch is slow because the gas adsorption-desorption process takes place with considerable amount of time.

In this study, ADR with passively operating fast heat switches are proposed and numerically investigated. A helium thermosyphon and a magneto-resistive tungsten are utilized as heat switches for the warm and cold ends, respectively. Both heat switches operate without involving any moving part, and passively change their heat transfer state according to the demand of the refrigeration system. Calculation results are presented and discussed; the used nomenclature is defined in Table 1.

## MATERIALS OF THE ADR

### Magnetic Material

The paramagnetic gadolinium gallium garnet ($Gd_3Ga_5O_{12}$, GGG) is selected as the magnetic material of the ADR. GGG is well known as the appropriate material for magnetic refrigeration at 2 K – 20 K range [8]. Total entropy of the magnetic material is the function of the temperature and the magnetic field, as shown in Equation 1.

$$\mathrm{ds} = \left(\frac{ds}{dT}\right)_H + \left(\frac{ds}{dH}\right)_T \tag{1}$$

Equation 1 can be converted to Equation 2 by the definition of the specific heat and the Maxwell relation.

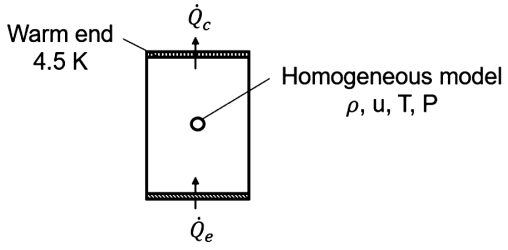


**Figure 1.** Schematics of the thermosyphon

$$\mathrm{ds} = \frac{c_H}{T} dT + \mu_o v \left(\frac{dM}{dT}\right)_H dH \tag{2}$$

Total entropy of the GGG can be obtained as shown in Equation 3 by integrating the Equation 2 if the specific heat at the zero field and the magnetization of the material are given in advance.

$$\mathrm{s(T, H)} = s_0 + \int_{T_0}^{T} \frac{c_{H=0}(T)}{T} dT + \mu_0 v \int_0^H \left[\left(\frac{\partial M}{\partial T}\right)_H\right]_T dH \tag{3}$$

Gallagher [9] presented the empirical correlations of the GGG entropy based on the experimental results of the previous studies which measured the specific heat and magnetization of the GGG. This study utilizes the Gallagher's correlation to simulate the magnetocaloric effect of the GGG. Specific heat of the GGG is calculated by differentiating the entropy, and the thermal conductivity is obtained from the study done by Daudin's group [10].

**Thermosyphon Heat Switch**

A Helium thermosyphon was selected as the heat switch for the warm side of the ADR. The Thermosyphon (Fig. 1) is a gravity-assisted heat transfer apparatus that has varying thermal conductance depending on the heat transfer mode of the working fluid inside of it. High thermal conductance between the evaporator and the condenser is accomplished if the phase change of the working fluid occurs inside of the thermosyphon, while heat is hardly transferred if the phase change doesn't occur. With this working principle, thermosyphon can be utilized as a heat switch by controlling the evaporator temperature above or below the saturation temperature of the working fluid. During the ADR cycle, the temperature of the GGG is varying due to the alternating field. The passive operation of the thermosyphon heat switch, thus, is accomplished by utilizing the GGG as the evaporator. The condenser of the thermosyphon maintains constant temperature by thermally connecting the condenser with the heat sink such as a cryocooler. During the magnetization process, the temperature of the GGG is increased and finally become higher than the saturation temperature of the working fluid. Subsequently, the thermosyphon turns on, GGG can effectively reject heat to the condenser. When the GGG is demagnetized, however, no more phase change occurs after the temperature of the GGG become lower than the saturation temperature. Therefore, heat leak from the warm condenser to the cold evaporator can be minimized. To simulate the operation of the thermosyphon, heat transfer coefficients of the helium are required. The boiling heat transfer coefficient of the helium is calculated by the Kutateladze correlation as shown in Equation 4, which was recommend by Smith [11]

$$\frac{h_e}{k_l}\left(\frac{\sigma}{g\rho_l}\right)^{1/2} = 3.25\times10^{-4}\left[\frac{\dot{Q}c_{p,l}\rho_l}{A_e i_{lg}\rho_g k_l}\right]^{1/3}\left[\frac{\dot{Q}c_{p,l}\rho_l}{A_e i_{lg}\rho_g k_l}\right]^{1/3}\left[g\left(\frac{\rho_l}{\mu_l}\right)^2\left(\frac{\sigma}{g\rho_l}\right)^{3/2}\right]^{1/8}\left[\frac{P}{(\sigma g\rho_l)^{1/2}}\right]^{1/8} \tag{4}$$

In the case of the condensation heat transfer coefficient, Nusselt's correlation [12] shown in Equation 5 is used.

$$h_c = \left[\frac{2\sqrt{2}}{3}\right]^{4/3} \cdot \left[\frac{{k_l}^3 g\rho_l(\rho_l - \rho_g) i_{lg} A_c}{\mu_l \dot{Q} L_c}\right]^{1/3} \tag{5}$$

**Table 2.** Constants of the Equation 7 [19]

| Constant | Value |
|---|---|
| $b_0$ | 0.03 |
| $a_1$ | 0.00025 |
| $a_2$ | 0 |
| $a_3$ | 1.1 |
| $a_4$ | 0.006 |
| n | 1.8 |

When the thermosyphon turns off, heat transfer between the evaporator and the condenser is accomplished by the conduction through wall and the working fluid. It is assumed that stainless steel consists the container of the thermosyphon, and the properties of the stainless steel are calculated by results provided from NIST [13]. Properties of the helium are calculated by the REFPROP 9.1 [14].

**Magnetoresistive Heat Switch**

Heat is conducted both by the lattice vibration (phonon) and the electron, as shown in Equation 6.

$$\mathrm{k} = k_{ph}(T) + k_{el}(T, B) \tag{6}$$

Thermal conduction by electron becomes dominant when the temperature is decreased below cryogenic temperature (<120 K). If the external magnetic field is exposed on a metal, heat diffusion by electron is suppressed and the thermal conductivity is reduced as a result. This phenomenon, magneto-resistive effect, can be applied to manufacturing a heat switch controlled by external magnetic field. Magneto-resistive effect is largely exhibited in the compensated metal with closed Fermi surface, and these materials such as gallium [15], cadmium [16], beryllium [17], and tungsten [18] were already studied for applying on heat switch. Tungsten is a good choice because it has low enough superconducting transition temperature (15 mK), so as it can be utilized in wide range of the temperature. Furthermore, it has the potential for achieving high on-off thermal conductance ratio because the Debye temperature of the tungsten is reasonably high (310 K). Magneto-resistive tungsten, thus, is selected as the heat switch for the cold side of the ADR. Hills [19] presented a phenomenological Equation of the tungsten's thermal conductivity by investigating the high purity (RRR>100,000) single crystal tungsten. This expression is shown in Equation 7 and the constants presented by the Hills are summarized in Table 2.

$$\mathrm{k} = b_0 T^2 + \frac{1}{\frac{a_1 + a_2 T^2}{T} + \frac{B^n}{a_3 T + a_4 T^4}} \tag{7}$$

With this equation, thermal conductivity of the tungsten under various temperature and magnetic field conditions is calculated in this study. In addition, specific heat of the tungsten is obtained from the Waite's study [20].

Alternating magnetic field variation is inevitably required in the ADR cycle. This study controls the cold side heat switch by exposing the tungsten with the same magnetic field exposed on the magnetic material of the ADR system. When the GGG rejects heat during the magnetization phase, thermal conductivity of the tungsten is reduced at the same time, and the heat leak from the GGG to the cold end is minimized, as a result. These situations are reversed during demagnetization phase. In conclusion, by exposing the same field variation on the magneto-resistive material with the magnetic material, passive operation is possible not only on the warm side thermosyphon, but also on the cold side heat switch.

**NUMERICAL ANALYSIS**

This study numerically investigates the performance and operational feasibility of the single stage ADR operating from 4.5 K to 2 K with passive heat switches. The analyzed ADR consists of GGG as the magnetic material, helium thermosyphon as the warm side heat switch, and tungsten as the cold side heat switch. Followings are the assumptions and the methods of the analysis.

1) It is assumed that the warm and the cold end of the ADR have infinite thermal capacitance and maintain constant temperature of 4.5 K and 2 K, respectively.

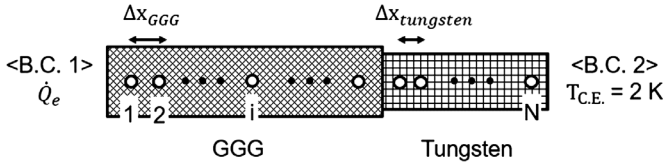


**Figure 2.** Grid system of the numerical analysis

2) The grid system of the GGG and the tungsten is set as shown in Figure 2. Heat transfer from the thermosyphon and the cold end temperature are set as the boundary conditions. One dimensional heat diffusion equation is solved during the analysis as shown in Equation 8.

$$\rho \mathrm{Ac}\frac{\partial \mathrm{T}}{\partial \mathrm{t}} = \mathrm{A}\frac{\partial}{\partial \mathrm{x}}\left\{\left(k\frac{\partial T}{\partial x}\right)\right\} - \mu_0\left(\frac{\partial M}{\partial T}\right)_H\left(\frac{dH}{dt}\right)TA \tag{8}$$

The rightmost term in Equation 8 represents the magnetocaloric effect, which is adapted only for the magnetic material. Thermal contact resistance [21] between the GGG and the tungsten is considered in the calculation. It is assumed that the tungsten is bonded to the GGG by epoxy (STYCAST 2850FT), because those materials have similar thermal expansion coefficient [22].

3) In the case of the thermosyphon as shown in Figure 2, the GGG and the warm end are utilized as the evaporator and the condenser of the thermosyphon, respectively. Since both the evaporator and the condenser are directly contacted with the fluid inside of the thermosyphon, perfect thermal contact condition is assumed in the analysis. Phase, pressure, and saturation temperature of the fluid inside of the thermosyphon should be calculated to simulate the operation of the thermosyphon. By using a homogeneous model, density and internal energy of the thermosyphon are calculated as shown in Equation 9 and 10.

$$\rho_{sys.} = \frac{m_{sys.}}{V_{sys.}} \tag{9}$$

$$m_{sys.}\frac{du}{dt} = \dot{Q}_e - \dot{Q}_c \tag{10}$$

$\dot{Q}_e$ and $\dot{Q}_c$ are obtained as shown in equation 11 and 12.

$$\begin{gathered}\text{when } T_{sat.} > T_{W.E.},\\ \dot{Q}_c = \mathrm{h}_c A_c (T_{sat.} - T_{W.E.})\\ \text{when } T_{sat.} \le T_{W.E.},\end{gathered} \tag{11}$$

The pressure and the saturation temperature of the thermosyphon is obtained from the internal energy and the density by using REFPROP 9.1. Amount of the liquid inside the thermosyphon is calculated by Equation 13.

$$\begin{gathered}\dot{Q}_c = \left\{\left(\frac{kA}{L/2}\right)_{fluid} + \left(\frac{kA}{L/2}\right)_{wall}\right\}(T_{sat.} - T_{W.E.})\\ \text{when } T_e > T_{sat.} \text{ and } m_l > 0,\\ \dot{Q}_e = \mathrm{h}_e A_e (T_e - T_{sat.})\\ \text{when } T_e \le T_{sat.} \text{ or } m_l = 0,\\ \dot{Q}_e = \left\{\left(\frac{kA}{L/2}\right)_{fluid} + \left(\frac{kA}{L/2}\right)_{wall}\right\}(T_e - T_{sat.})\end{gathered} \tag{12}$$

$$m_l = \rho_l \frac{\rho_{sys.} - \rho_g}{\rho_l - \rho_g} V_{sys} \tag{13}$$

The equivalent thermal conductivity of the thermosyphon, $k_{fluid}$, is obtained as shown in Equation 14.

$$k_{fluid} = \frac{(m_l/\rho_l)k_l + (m_g/\rho_g)k_g}{V_{sys.}}, \text{ where } m_g = m_{sys.} - m_l \tag{14}$$

**Table 3.** Operating conditions of the numerical analysis

| Operating conditions | |
|---|---|
| Warm end temperature | 4.5 K |
| Cold end temperature | 2 K |
| Initial temperature | 4.5 K |
| Initial filling ratio (thermosyphon) | 30 % |
| Maximum field | 3 T |
| Magnetization speed | 0.2 T/s |
| Demagnetization speed | -0.2 T/s |
| Heat absorption process | until $T_{GGG}$ < 1.8 K |

**Table 4.** Dimensions of the analyzed system

| Thermosyphon (cylinder) | |
|---|---|
| Inner diameter | 21 mm |
| Thickness | 0.3 mm |
| Length of adiabatic region | 20 mm |
| Condenser length | 5 mm |
| Condenser area | 330 $mm^2$ |
| Evaporator area | 346 $mm^2$ |
| Volume | 8,650 $mm^3$ |
| **GGG (cylinder)** | |
| Diameter | 21 mm |
| height | 30 mm |
| **Tungsten (wire cut disk)** | |
| Conduction area | 2.25 $mm^2$ |
| Effective conduction length | 50 mm |
| Contact area with the GGG | 69 $mm^2$ |

4) Table 3 summarizes the conditions of the analysis. The initial conditions are set as the whole system maintains the temperature of the warm end. In addition, it is assumed that the liquid firstly fills the 30% of the total volume of the thermosyphon before the ADR cycle starts. Maximum magnetic field and ramp rate is set as 3 T and ±0.2 T/s, respectively. Those parameters are decided by considering the specification of the conduction-cooling HTS magnet [23]. The heat absorption process is set to proceed until the GGG maintains more than 0.2 K temperature difference with the cold end. Dimensions of the system are also summarized in Table 4. In the case of the tungsten, it is assumed that the tungsten heat switch is made from wire cut tungsten single crystal with diameter of 10 mm and height of 5 mm. Conduction area of the tungsten ($(1.5\ mm)^2$) is determined with the consideration of electron mean free path of the high purity tungsten [24]. In addition, some part of the tungsten is utilized as the contact area with the GGG to minimize the thermal contact resistance. Remaining part of the tungsten, thus, is utilized as the effective length for thermal conduction.

## RESULTS AND DISCUSSION

Figure 3 shows the calculation result of the ADR cycle after reaching cyclic steady state. As shown in the figure, according to the alternating field, the temperature of the GGG also changes periodically by magnetocaloric effect. The regeneration time is calculated as 30 s, which is defined as sum of the time

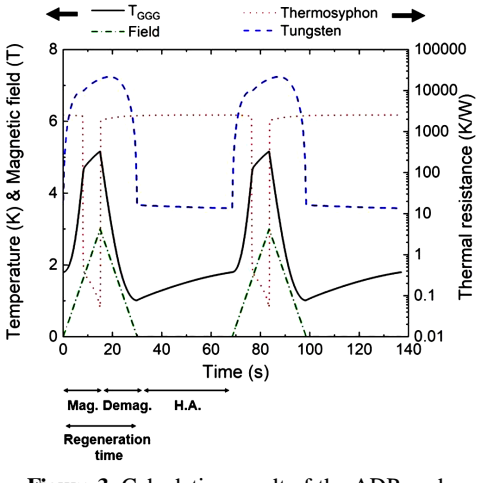


**Figure 3.** Calculation result of the ADR cycle

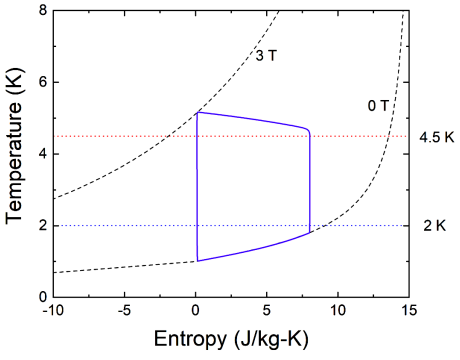


**Figure 4.** T-s diagram of the GGG

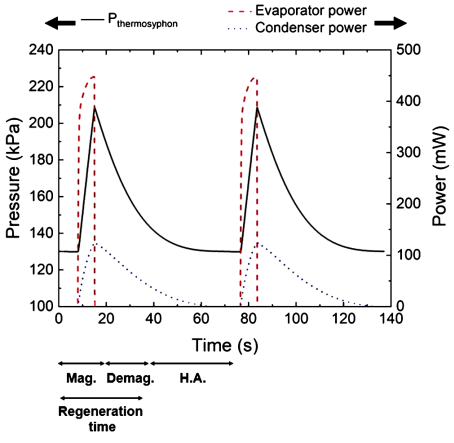


**Figure 5.** Variation inside the thermosyphon during the ADR cycle

required for the magnetization and the demagnetization process. In addition, the thermal resistance of the heat switches are also varied as shown in the figure. States of the switches (on and off) are passively determined by the temperature of the GGG and the external magnetic field. The on-off ratios of the warm and the cold side heat switch, as defined in Equation 15, are calculated as 49300 and 1600, respectively.

$$on - off\ ratio = \frac{R_{max.}}{R_{min.}} \tag{15}$$

In the case of the warm side, heat of 2.87 J is rejected from the GGG to the evaporator at the regeneration process, while heat of 0.05 J is leaked from the warm end to the GGG at the heat absorption process. In the case of the cold side heat switch, heat of 3 mJ is leaked from the GGG to the cold end at the regeneration process, while heat of 0.773 J is absorbed from the cold end to the GGG at the heat absorption process.

This study confirms that the GGG reaches below 1 K after demagnetization, and successfully absorbs the heat from 2 K cold end. Cooling capacity and the COP of the ADR are calculated as 0.770 J and 0.376, respectively. The T-s diagram of the GGG during the refrigeration cycle is also shown in Figure 4. The operation of the ADR with passive heat switches, thus, is confirmed to be feasible.

Figure 5 shows the variation inside the thermosyphon during the ADR cycle. Pressure inside the thermosyphon changes due to the evaporated helium by the GGG and the condensed helium by the warm end. The calculated pressure, which is equivalent to the saturation temperature, decides the heat transfer coefficients at the evaporator and the condenser. The heat rejected from the evaporator is exactly same as the heat absorbed from the condenser. It is identified that the generated heat from the GGG during the regeneration time is effectively rejected to the warm end through the thermosyphon.

The ADR with passive heat switches in this study has inherently lower efficiency than that of the ADR with active heat switches. The theoretical capacity of the ADR is calculated as shown in Equation 16.

$$\frac{Q_{ideal}}{m} = s(T_{C.E.}, 0) - s(T_{W.E.}, B_{max.}) \tag{16}$$

The theoretical capacity of the ADR in this study is calculated as 1.16 J, thus, 67% of the ideal capacity is accomplished with the passive heat switches. Most of the irreversibility is originated from the temperature difference between the GGG and the cold end during the heat absorption process. The tungsten heat switch turns on when the external magnetic field is entirely removed. Therefore, heat cannot be absorbed isothermally by controlling the demagnetization rate. Consequently, perfect Carnot cycle cannot be accomplished with ADR in this study. The passive heat switch, though, still is attractive because it can operate without any control system simplifying the whole refrigeration system.

## CONCLUSION

The adiabatic demagnetization refrigerator (ADR) is proposed with passive heat switches and its performance is numerically predicted. A helium thermosyphon and a magneto-resistive tungsten are utilized as heat switches for the warm and the cold ends, respectively. Both heat switches passively change their states according to change of refrigeration cycle. The warm end of the ADR is set to maintain at 4.5 K and the bottom of the thermosiphon (cold end) is set to maintain at 2 K. This study numerically identifies that the GGG can reach below 1 K after demagnetization, and successfully absorbs the heat from 2 K cold end. In addition, the cooling capacity and the COP of the ADR are calculated as 0.770 J and 0.376, respectively. The operation of the ADR with passive heat switches, which does not require any control systems for the heat switches, is confirmed to be feasible.

## ACKNOWLEDGMENT

This research was supported by Basic Science Research Program through the National Research Foundation of Korea (NRF-2017R1A2B3003152) funded by the Ministry of Science, ICT & Future Planning (MSIP).

## REFERENCES

1. Giauque, W. F., "Paramagnetism and the third law of thermo-dynamics. interpretation of the low-temperature magnetic susceptibility of gadolinium sulfate.", *Journal of the American Chemical Society,* 49, 8 (1927), pp. 1870-1877.
2. Debye, P., "Einige bemerkungen zur magnetisierung bei tiefer temperatur.", *Annalen der Physik,* 386, 25 (1926), pp. 1154-1160.
3. Giauque, W. F., and D. P. MacDougall, "Attainment of Temperatures Below 1° Absolute by Demagnetization of Gd 2 (S O 4) 3· 8 H 2 O.", *Physical Review,* 43, 9 (1933), pp. 768.
4. Bywaters, R. P., and R. A. Griffin. "A gas-gap thermal switch for cryogenic applications." *Cryogenics* 13.6 (1973): 344-349.
5. Frank, D. J., and T. C. Nast, "Getter-activated cryogenic thermal switch.", *Advances in cryogenic engineering*, Springer, Boston, MA (1986), pp. 933-940.
6. DiPirro, M. J., et al., "Design and test of passively operated heat switches for 0.2 to 15 K.", *AIP Conference Proceedings*, vol. 710, no. 1 (2004), pp. 436-442.
7. Kimball, Mark O., et al., "Passive gas-gap heat switches for use in low-temperature cryogenic systems.", *IOP Conference Series: Materials Science and Engineering*, vol. 278, no. 1 (2017), pp. 012010.
8. Barclay, J. A., and W. A. Steyert, "Materials for magnetic refrigeration between 2 K and 20 K.", *Cryogenics,* 22, 2 (1982), pp. 73-80.
9. Gallagher, Gregory Roy, *Analysis of a magnetically active regenerator*, Diss., Massachusetts Institute of Technology (1986)
10. Daudin, B., R. Lagnier, and B. Salce, "Thermodynamic properties of the gadolinium gallium garnet, Gd3Ga5O12, between 0.05 and 25 K.", *Journal of Magnetism and Magnetic Materials,* 27, 3 (1982), pp. 315-322.
11. Smith, R. V., "Review of heat transfer to helium I.", *Cryogenics,* 9, 1 (1969), pp. 11-19.
12. Bergman, T. L., Incropera, F. P., DeWitt, D. P., & Lavine, A. S., "Fundamentals of heat and mass transfer*"*. John Wiley & Sons (2011).
13. Marquardt, E. D., Le, J. P., & Radebaugh, R.. "Cryogenic material properties database.". In *Cryocoolers, 11*, Springer, Boston, MA (2002), pp. 681-687.
14. Lemmon, E. W., Huber, M. L., & McLinden, M. O. (2013). NIST standard reference database 23: reference fluid thermodynamic and transport properties-REFPROP, version 9.1, standard reference data program. *National Institute of Standards and Technology: Gaithersburg, MD.*

15. Engels, J. M. L., Gorter, F. W., & Miedema, A. R.. “Magnetoresistance of gallium—A practical heat switch at liquid helium temperatures.”, *Cryogenics*, 12*,* 2 (1972), pp. 141-145.

16. Laudy, J., and Knol, A., “A cadmium heat switch.”, *Cryogenis*, 6*.* 6 (1966), pp. 370-371.

17. Radebaugh, R., “Electrical and thermal magnetoconductivities of single-crystal beryllium at low temperatures and its use as a heat switch.”, *Journal of Low Temperature Physics*, 27*,* 1-2 (1977), pp. 91-105.

18. Bartlett, J., Hardy, G., Hepburn, I., Ray, R., and Weatherstone, S.. “Thermal characterisation of a tungsten magnetoresistive heat switch.”, *Cryogenics*, 50, 9 (2010), pp. 647-652.

19. Hills, M. J., ”Thermal Transport in Tungsten and Applications to Miniaturised Adiabatic Demagnetisation Refrigerators”, Diss., UCL (University College London) (2016)

20. Waite, T. R., Craig, R. S., and Wallace, W. E., “Heat Capacity of Tungsten between 4 and 15 K.”, *Physical Review*, 104, 5 (1956), pp. 1240.

21. Gmelin, E., Asen-Palmer, M., Reuther, M., and Villar, R., “Thermal boundary resistance of mechanical contacts between solids at sub-ambient temperatures.”, *Journal of Physics D: Applied Physics*, 32*,* 6 (1999), R19.

22. Shirron, P. J., and McCammon, D., “Salt pill design and fabrication for adiabatic demagnetization refrigerators.”, *Cryogenics*, 62 *(2014)*, pp. 163-171.

23. J. Park, I. Park, S. Jeong and S. Kim, “Experimental investigation on conduction-cooled fast-ramping layer-wound (RE)BCO superconducting magnet for magnetic refrigeration”, *IEEE Trans. Appl. Supercond.*, vol. 24, no. 3 (2015)

24. Canavan, E. R., Dipino, M. J., Jackson, M., Panek, J., Shirron, P. J., and Tuttle, J. G., “A magnetoresistive heat switch for the continuous ADR.”, In *AIP Conference Proceedings,* vol. 613, no. 1 (2002), pp. 1183-1190.